THE BELL SYSTEM TECHNICAL JOURNAL
Vol. 57, No. 3, March 1978
Printed in U.S.A.

Polarization Effects in Short Length, Single Mode Fibers

By V. RAMASWAMY, R. D. STANDLEY, D. SZE, and W. G. FRENCH

(Manuscript received December 14, 1976)

The ability to maintain linearly polarized output in single mode fibers is essential for utilization of polarization dependent receiver circuitry. Our measurements with long lengths of fiber (200 m) indicate that we can find input polarization angles which yield essentially linearly polarized output. However, we found that these polarization effects are greatly influenced by the presence of physical stress on the fiber such as stress due to bending, twisting, mounting, and other variations in ambient conditions. We conducted several experiments on short length fibers where special precautions were adopted to assure repeatability of the measurements. Our results indicate the existence of a general theoretical model that predicts the output polarization characteristics as a function of input polarization and fiber length. The model assumes the presence of two asynchronous, orthogonal modes, uniformly coupled over the entire fiber length. The model, however, cannot distinguish between uniformly coupled and uncoupled mode cases based on the output radiation measurements.

I. INTRODUCTION

The polarization characteristics of "single" mode optical fibers have been the subject of several previous publications.[1,2] An understanding of the polarization sensitivity of such fibers is important in assessing the applicability of polarization dependent optical circuitry.[3] An additional implication of polarization sensitivity is the introduction of delay distortion in "single" mode fibers.

In this paper, we present a theoretical model based on the propagation of two orthogonal modes; it is shown that based on the measurement of

the ellipticity of the output radiation alone, we cannot distinguish between the following cases:

(*i*) The existence of two orthogonal modes, uncoupled with different propagation constrants.

(*ii*) The existence of two orthogonal modes, with identical propagation constants and uniformly coupled by some means of periodic perturbation

(*iii*) The most general case—two orthogonal modes, uniformly coupled, but with nonidentical propagation constants.

The organization of the paper is as follows. In Section II, we summarize the theory, leaving the details to the Appendices. Section III describes the detailed experimental procedure utilized to measure the radiation ellipse as well as details of each of the measurements. In Section IV the experimental data is compared with simple theoretical results developed in Section II.

It should be noted that the assumption of synchronous uncoupled modes will not verify our data. An additional finding of importance is that the most general case indicates that for a fiber of any given length, excitation conditions exist at the input that result in linearly polarized output.

II. THEORETICAL MODEL

For completeness, we state the obvious: for synchronous uncoupled modes, the output radiation would be linearly polarized independent of the orientation of linear input polarization and fiber length. Experimentally, this is not observed and, hence, this model is ruled inappropriate.

As detailed in Appendices B and C, we assume spatially orthogonal modes whose propagation constants differ by $\Delta\beta$; we further assume that the modes are uniformly coupled with a constant coupling κ. The fiber output radiation ellipse,[4] as described in Appendix A, would possess the following characteristics. If a and b are the amplitudes of the semi-major and minor axis components of the radiation ellipse, then their ratio is

$$R = \pm \frac{a}{b} = \frac{1 \pm [1 - \sin^2 2\theta' \sin^2 2\alpha]^{1/2}}{\sin 2\theta' \sin 2\alpha} \tag{1}$$

and the orientation ψ of the major axis of the ellipse is

$$\psi = 1/2 \tan^{-1} (\tan 2\theta' \cos 2\alpha) - \eta/2 \tag{2}$$

where $\theta' = \theta + \eta/2$

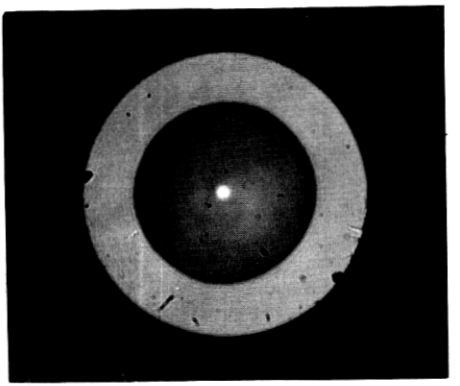

Fig. 1—Photomicrograph of single mode fibers, core diameter = 4.7 μ, outside diameter = 133 μ.

θ = input orientation of polarization with respect to x axis
$\eta = \tan^{-1} 2\kappa/\Delta\beta$
$\alpha = 1/2\sqrt{\Delta\beta^2 + 4\kappa^2}\, z$
z = fiber length

When $R = 0$ or ∞, the output is linearly polarized. From eq. (1), we see that this happens at $\theta' = \pm m\pi/2$, independent of fiber length. Thus, this model predicts that even in the presence of either phase asynchronism or mode coupling (or both), there are specific orientations of input polarization,

$$\theta = -\eta/2 \pm m\pi/2 \tag{3}$$

for which linear polarization is observed for all lengths. The measured relative phase shift $2\alpha = \sqrt{\Delta\beta^2 + 4\kappa^2}\, z$, can be thought of as due to an effective $\Delta\beta_e$ that includes the effect of coupling such that

$$\Delta\beta_e = \sqrt{\Delta\beta^2 + 4\kappa^2} \tag{4}$$

In our measurements, the reference angle $\theta' = 0$ was always selected at first by rotating the input polarization to that angle for which the output was linearly polarized; then based on the observations of the radiation ellipse at the output, we cannot distinguish between the following cases: (*i*) asynchronous, uncoupled modes, (*ii*) synchronous, coupled modes, and (*iii*) asynchronous, coupled modes. These cases are summarized in Table I.

III. EXPERIMENTAL PROCEDURE

Figure 1 shows a photomicrograph of the fiber when illuminated with white light. The fibers used had a core of pure SiO_2 and a cladding of

Table I—Summary of cases

Case	2α	$\theta' = 0$ (reference) at	$R = \frac{a}{b}$	ψ
Asynchronous ($\Delta\beta \neq 0$) Uncoupled ($\kappa = 0$)	$\Delta\beta z$	$\theta = 0$	$\frac{1 \pm \sqrt{1 - \sin^2 2\theta \sin^2 2\alpha}}{\sin 2\theta \sin 2\alpha}$	$\frac{1}{2}\tan^{-1}[\tan 2\theta \cos 2\alpha]$
Synchronous ($\Delta\beta = 0$) Uniformly coupled ($\kappa \neq 0$)	$2\kappa z$	$\theta = -\pi/4$	Same as above with θ replaced by θ'; θ rotated by $-\pi/4$	
Asynchronous $\Delta\beta \neq 0$ Uniformly coupled ($\kappa \neq 0$)	$\Delta\beta_e z = \sqrt{\Delta\beta^2 + 4\kappa^2}\, z$	$\theta = -\eta/2$	Same as above with θ replaced by θ'; now θ rotated by $-\eta/2$	

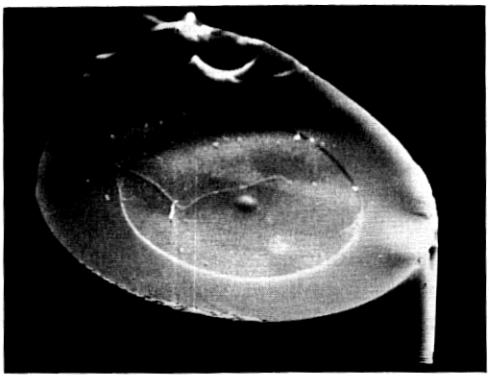

Fig. 2—Electron micrograph of etched single mode fiber.

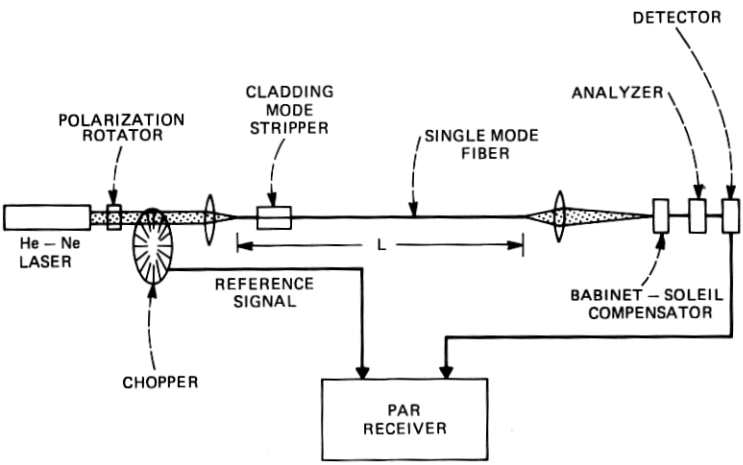

Fig. 3—Experimental set-up.

$B_2O_3 \cdot 6SiO_2$. The core and the outer diameters were 4.7 μm and 133 μm, respectively. Due to diffusion of B_2O_3 in the MCVD fabrication process, the fiber core was unintentionally graded in refractive index and the Δn was lower than expected for these compositions.[5] Figure 2 shows an electron micrograph of the etched fiber.[6] The effective core-cladding index difference was $\Delta n \approx 2 \times 10^{-3}$. Fibers of lengths usually less than 3 meters were used in our short fiber length measurements.

The experimental arrangement is shown in Fig. 3. Light from a polarized He-Ne laser is passed through a polarization rotator to facilitate rotation of the input polarization at the input of the fiber. The light was chopped to provide a reference signal at the receiver and then focused

on the fiber by means of a lens. A small section of the fiber near the input end was immersed in glycerol to remove any undesired cladding mode that might have been excited. The output light was collimated by a lens and passed through a Glan-Thomson analyzer before being detected and displayed in a PAR receiver. A Babinet-Soleil compensator could be inserted and removed, as needed, between the collimating lens and the analyzer.

Experimentally, we found the polarization effects on long and short length fibers were greatly influenced by the presence of any stress on the fiber and other changes in ambient conditions. To ensure repeatability of the measurement, it was necessary to take many precautions. The fibers were held as straight as possible by gently taping them on to a flat surface, at regular but not necessarily identical intervals to minimize inducing any stress in the fiber. The input end of the fiber was held by using a vacuum chuck except in one experiment where it was held by a mechanical holder. In that case, it was clamped first using as little pressure as possible and then taped. In all our measurements, the input polarization angle, which resulted in linearly polarized output, served as the input reference angle, i.e., $\theta' = 0$. The analyzer position oriented to measure the cross polarized component served as the reference axis for the orientation of the output ellipse. If we alter the angle θ', the output in general will become elliptically polarized. In order to obtain the phase difference δ between components parallel and perpendicular to the reference angle $\theta' = 0$, we have to orient the Babinet-Soleil compensator parallel or perpendicular to the original reference axis of the analyzer. With the plunger of the compensator adjusted to obtain linear polarization at the output, from the plunger position and the calibration of the compensator, the phase shift 2α can then be calculated. In each measurement, where input polarization is rotated with a given fixed length of the fiber, or where the length of the fiber is varied keeping the input excitation angle θ' fixed, the output analyzer was oriented parallel to the major and minor axis of the output ellipse to obtain the power ratio of these components. Orientation of the minor axis was also determined from the angular position of the analyzer.

IV. EXPERIMENTAL RESULTS

4.1 Fixed fiber length, input polarization varied

In this experiment, an input reference angle was found such that the output polarization was linearly polarized; we then measured the ellipticity of the output radiation as a function of input polarization rotation about this reference. Figures 4 and 5 compare the experimental data with the theoretical results obtained by computing $20 \log_{10} R$ from eq. (1) and evaluating the orientation of eq. (2). The best fit was for $2\alpha = 59°$, which

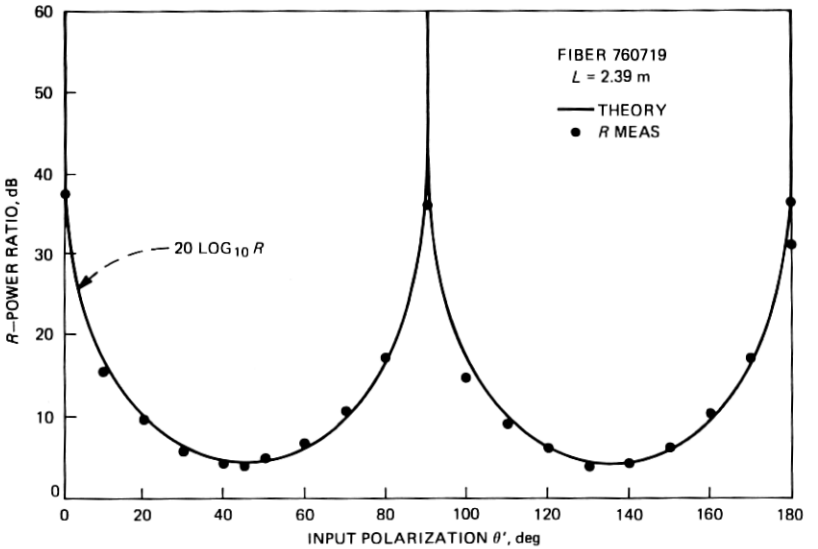

Fig. 4—Measured and theoretical power output ratio, R, of the major to minor axis components of output radiation ellipse as a function of input polarization angle (θ'). Fiber length L = 2.39 meters.

was also verified from the compensator measurement. However, this experiment cannot give a specified value for the phase retardation per unit length, i.e., $\delta/L(=\Delta\beta_e)$, since we can not determine explicitly the integral number of $\pi/2$ phase shifts included in the entire length of the fiber.

4.2 Fixed input polarization, variable length

4.2.1 On axis excitation ($\theta' = 0$)

In this experiment, after finding the reference axis, orientation and power ratio R of the output ellipse was measured; the fiber was shortened at the input end repeatedly by a small amount ($\approx$ 5 mm) and the experiment was repeated by reorienting the input polarization to obtain a linearly polarized output. From Fig. 6, we infer, as the theory predicts, essentially a linearly polarized output independent of the fiber length. The experimental limit of 38 dB indicated in the figure is the limitation imposed by the degree of polarization of the laser source. Our measurements on long lengths ($\approx$200 m) indicate the cross polarized component was down 32 dB. However, the output polarization was subject to severe variations due to physical stress and other changes in ambient conditions.

The data (not shown) indicate the input polarizer angle and the output

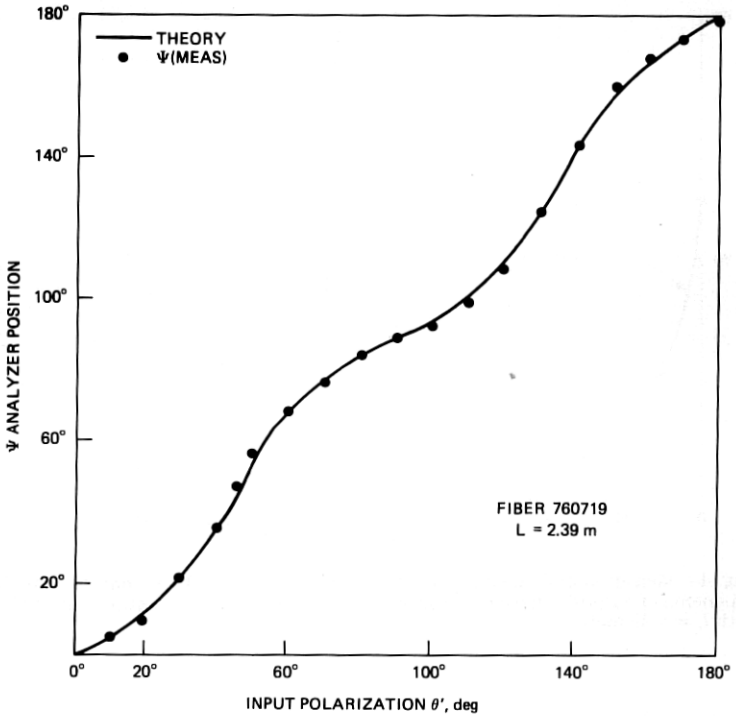

Fig. 5—Measured and estimated relative orientation of the ellipse ψ as a function of input polarization angle θ' for $L = 2.39$ meters.

analyzer angle remained essentially unchanged with deviations, within experimental errors, indicating negligible angular rotation of the fiber with length.

4.2.2 *Slightly off-axis excitation* ($\theta' \approx 6°$)

This experiment was conducted by offsetting the input polarization by an angle θ' ($\approx 6°$). The input fiber end was held mechanically; the output end was successively cut and the measurements were repeated. As expected the output was elliptically polarized; as a function of length, the polarization changes from elliptical to linear and then back to elliptical. From eq. (3) for a small angular offset, i.e., for small θ'

$$|R| \approx \frac{1}{\sin 2\alpha} \tag{5}$$

and from (4)

$$\psi = \frac{1}{2}\tan^{-1}[2\theta' \cos 2\alpha]$$
$$\approx \theta' \cos 2\alpha \tag{6}$$

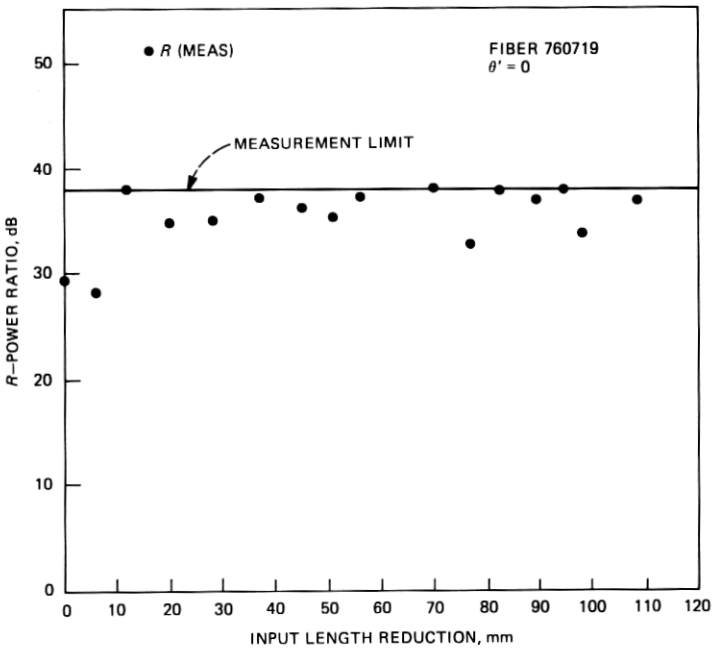

Fig. 6—Essentially linear polarization is observed at the output when input end is shortened with on axis ($\theta' = 0$) excitation.

Figure 7 shows the excellent agreement between theory and experiment. In fitting the ψ data, it was necessary to include a "twist" term of the order of 0.16°/mm. This implied a periodicity of the twist to be about 2.25 m, which is very close to the length of the fiber and was traced later to the holding and mounting arrangement at the input end of the fiber. When the fiber was allowed to lie flat and straight, and the input end was held using a vacuum chuck, the twist disappeared.

From the compensator measurements after each cut, the average $\Delta\beta_e$ was evaluated to be $\approx$0.0581 radians per mm. As seen from Fig. 7, linear polarization occurs at about every 54 mm and from eq. (5), it is obvious that this occurs when $2\alpha = 0, \pi, \ldots$ etc. Therefore $2\alpha = \Delta\beta L = \pi$ with the result $\Delta\beta_e = 0.0582$ radians per mm, in agreement with the compensator measurements. This leads to an estimated value of effective index difference

$$\Delta n_e = \frac{\Delta\beta_e}{2\pi}\lambda = \frac{\lambda}{2L} = 5.86 \times 10^{-6}$$

between the modes. Thus, it seems reasonable to state that the fibers cannot be easily fabricated to such tolerances and, hence, the polarization

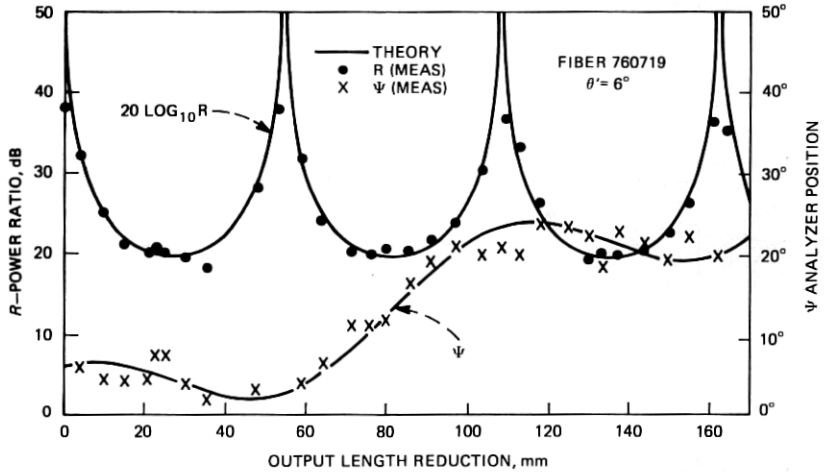

Fig. 7—Analytical predictions that R varies as $(\theta' \sin 2\alpha)^{-1}$, and ψ varies as $(\theta' \cos 2\alpha)$ as a function of length for small θ', confirmed experimentally. Period between successive linear polarization is 54 mm yielding a $\Delta\beta = 0.0582$ radians/mm.

problems observed with these experimental fibers will qualitatively be observed for all nominally circular, single mode fibers.

4.2.3 Excitation at $\theta' = \pi/4$

If the fiber was excited at 45° from the reference angle $\theta' = 0$, two modes of equal amplitudes would be excited; at the fiber output they would be out of phase by $2\alpha = \Delta\beta_e L$. Therefore in this case, the polarization will change, as a function of length, from circular to linear and then back to circular with elliptical polarization in between. For $\theta' = \pi/4$, from eq. (1) and (2),

$$|R| = \frac{1}{\tan \alpha}, \tag{9}$$

and

$$\psi = \pm\pi/4 \tag{10}$$

In eq. (4), when $\cos 2\alpha$ goes through zero, i.e., at $\alpha = \pi/4$ and $|R| = 1$ (circular polarization), ψ changes sign. Experimental results compare very well with the analysis as shown in Fig. 8.

V. CONCLUSIONS

The fibers used in these experiments were nominally circularly symmetric; however, the data on the elliptically polarized output radiation indicates that very small deviations from circular symmetry possibly exist and that these irregularities cause serious polarization effects. It

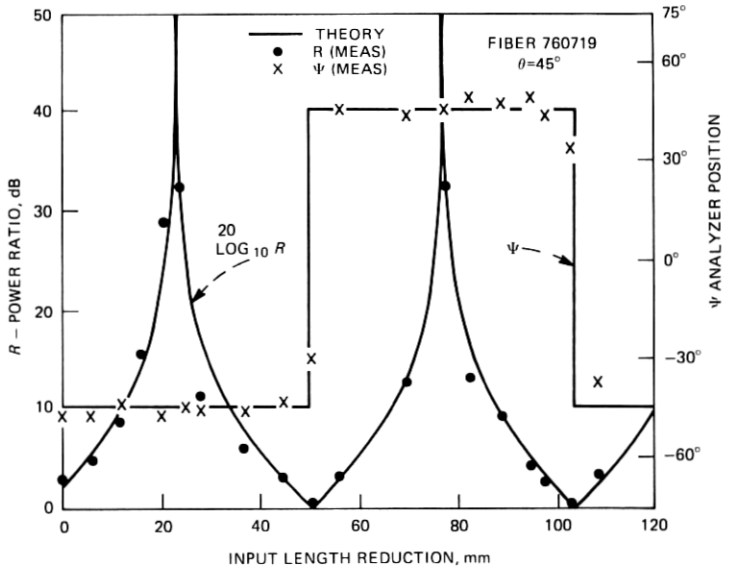

Fig. 8—Behavior of output polarization with decreasing input length. R varies as $(\tan \alpha)^{-1}$ and $\psi = \pm 45°$. The beat period is the same as before—54 mm.

appears unlikely that the fiber fabrication process can be improved to the extent that such effects can be completely eliminated.

The results indicate that input excitation conditions do exist for which linearly polarized output will be observed for a fiber of any length. However, the output polarization is subject to severe variations due to physical stress and other changes in ambient conditions. Our experiments can not determine whether any mode coupling exists. However, if any mode coupling exists, it must be uniform, at least over the few meter lengths of the fiber measured.

Polarization behavior of single mode fibers may hopefully be improved, by making the cores purposely elliptical, provided that any periodic perturbation such as "twisting" of the core is sufficiently small and does not result in strong mode coupling. Large ellipticity, however, will increase the modal dispersion. Further study is necessary to characterize the polarization behavior of elliptical core fibers and, if they hold polarization, to arrive at an optimum degree of ellipticity that would provide a balance between polarization control and dispersion effects.

VI. ACKNOWLEDGMENTS

The authors are grateful to E. A. J. Marcatili and D. Gloge for useful discussions and to P. Kaiser for drawing the fibers used in the experiment.

APPENDIX A

Orientation and Ratio of Major to Minor Axis of Vibrational Ellipse of Elliptically Polarized Waves

Consider two time-varying (S.H.) orthogonal electric field components

$$E_x = a_1 e^{j(\omega t + \delta_1)} \tag{11}$$

$$E_y = a_2 e^{j(\omega t + \delta_2)} \tag{12}$$

such that $a_1^2 + a_2^2 = 1$. The resulting electric vector, as seen from Fig. 9, traces, in general, an ellipse. The difference in the effective propagation constants between the two waves is

$$\Delta\beta = \frac{\beta_1 - \beta_2}{L} = \frac{\delta}{L} \tag{13}$$

where L is the fiber length. Whenever a_1 or a_2 is zero or when $\delta = m\pi$, where m is an integer, the output wave is linearly polarized. Furthermore, when $a_1 = a_2$, and $\delta = (2m + 1)\pi/2$, the output is circularly polarized. The ratio R of the semi-major to semi-minor axis of the ellipse can be defined as[4]

$$R = \frac{a}{b} = \tan \chi \tag{14}$$

where χ is an auxiliary angle ($-\pi/4 \leq \chi \leq \pi/4$). By choosing an angle $\phi (0 \leq \phi \leq \pi/2)$ such that

$$\tan \phi = \frac{a_2}{a_1} \tag{15}$$

the angle ψ of the orientation of the resultant ellipse, with respect to a reference axis ox, and the parameters ϕ and χ are related by[4]

$$\sin 2\chi = \sin 2\phi \sin \delta \tag{16}$$

$$\tan 2\psi = \tan 2\phi \cos \delta \tag{17}$$

In addition,

$$a_1^2 + a_2^2 = a^2 + b^2 \tag{18}$$

By eliminating χ from equations (14) and (16), and with the use of eq. (15), we find

$$R = \pm\frac{a}{b} = \frac{1 \pm \sqrt{1 - 4a_1^2 a_2^2 \sin^2 \delta}}{2a_1 a_2 \sin \delta} \tag{19}$$

and from eqs. (17) and (15),

$$\psi = \frac{1}{2} \tan^{-1} \left[\frac{2a_1 a_2}{a_1^2 - a_2^2} \cos \delta \right] \tag{20}$$

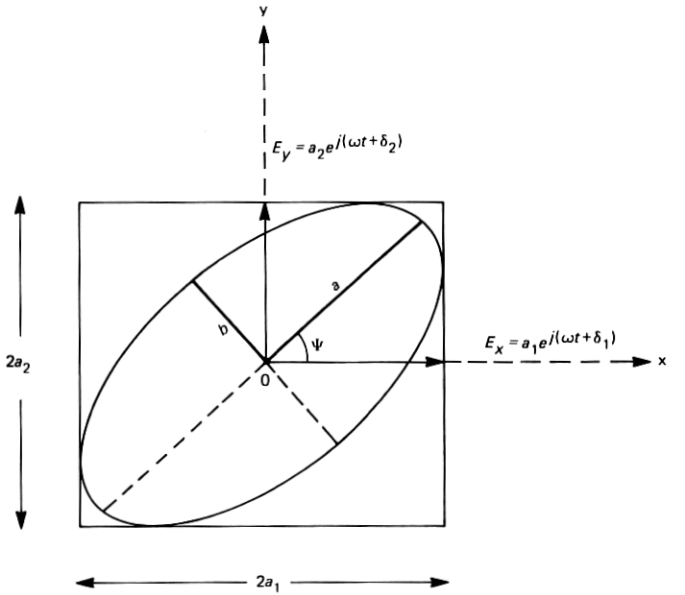

Fig. 9—Output radiation ellipse.

APPENDIX B

Relations Between Input Polarization Angle, Fiber Parameters, and Output Ellipse

We assume a cartesian co-ordinate system, as shown in Fig. 10, with ox and oy coincident with the axes of slightly elliptical core or with that of the birefringent axes of the core of a single mode fiber as the case may be. Let us also assume that a linearly polarized plane wave is incident upon the fiber at an angle θ with respect to ox; therefore the amplitudes of the excited modes with orthogonal polarization are $\cos\theta$ and $\sin\theta$ and represent the x and y component respectively.

Assuming a uniformly distributed coupling characterized by a coupling constant κ between the modes whose propagation constant differ by $\Delta\beta$, the complex field amplitudes are given by[7,8]

$$E_x = \cos\theta \cos\alpha - j \cos(\eta + \theta) \sin\alpha \tag{21}$$

$$E_y = \sin\theta \cos\alpha + j \sin(\eta + \theta) \sin\alpha \tag{22}$$

where the parameter α, proportional to the length of the fiber, is

$$\alpha = \sqrt{(\Delta\beta/2)^2 + \kappa^2}\, z \tag{23}$$

and the parameter η which relate the degree of coupling and the asynchronism between modes is given by

$$\tan\eta = 2\kappa/\Delta\beta \tag{24}$$

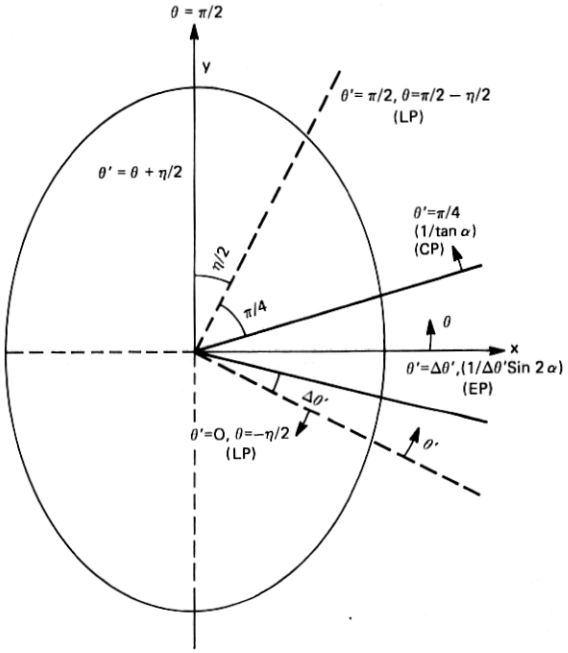

Fig. 10—Input excitation conditions and the behavior of the resulting output polarization.

For reasons indicated in the text, we exclude the case when both κ and $\Delta\beta$ are equal to zero. For the case $\kappa = 0$ and $\Delta\beta$ finite, η equals zero. If $\Delta\beta = 0$ and κ is finite, η equals $\pi/2$. When both κ and $\Delta\beta$ are finite, $0 \leq \eta \leq \pi/2$.

By rewriting eqs. (21) and (22) similar to eqs. (11) and (12), we see that

$$a_1^2 = \cos^2\theta \cos^2\alpha + \cos^2(\eta + \theta) \sin^2\alpha \tag{25}$$

$$a_2^2 = \sin^2\theta \cos^2\alpha + \sin^2(\eta + \theta) \sin^2\alpha \tag{26}$$

and

$$a_1^2 - a_2^2 = \cos 2\theta \cos^2\alpha + \cos 2(\eta + \theta) \sin^2\alpha \tag{27}$$

The phase constant δ is determined by

$$\tan\delta = \frac{2 \sin(2\theta + \eta) \tan\alpha}{\sin 2\theta - \sin 2(\theta + \eta) \tan^2\alpha} \tag{28}$$

Substituting (25) through (28) in (19) and (20) we find, after considerable trigonometric manipulation, that the ratio of the major to minor axis

of the resultant output ellipse is

$$R = \frac{1 \pm [1 - \sin^2 (2\theta + \eta) \sin^2 2\alpha]^{1/2}}{\sin (2\theta + \eta) \sin 2\alpha} \tag{29}$$

and its orientation

$$\psi = \frac{1}{2} \tan^{-1} [\tan (2\theta + \eta) \cos 2\alpha] - \frac{\eta}{2} \tag{30}$$

By appropriate choice of the sign, we see that $|R|$ in eq. (29) is bounded by 1 and ∞ or 0 and 1. Whenever $|R|$ goes to 0 or ∞, we have linear polarization. For a given length of the fiber z, therefore α, this occurs when

$$\theta = -\frac{\eta}{2} \pm m \frac{\pi}{2}, \; m = 0, 1, 2, \ldots \tag{31}$$

As η varies from 0 to $\pi/2$, the input angle θ at which the output is linearly polarized varies from 0 to $-\pi/4$. In the most general case, at this specific angle, phase difference δ, as seen from equation (28), equals either zero or multiples of π and is independent of α indicating that the two modes are either in or out of phase with each other at the output for all lengths. This clearly shows for a given fiber with a finite κ and $\Delta\beta$, there is always an orientation of input polarization that would result in a linear polarization at the output.

Note that in the special case $\eta = 0$, $\delta = 2\alpha$ and therefore, δ is dependent on length; however, at $\theta = \pm m\pi/2$, as seen from (25) and (26), one of the components goes to zero. Thus the condition for input excitation angle θ to achieve linear polarization at the output, for all values of α, is given by (31) and holds good for all values of η in the range $0 \leq |\eta| \leq \pi/2$.

APPENDIX C

General Theoretical Model Used for Observation of Output Ellipticity

In this Appendix, we consider the general case illustrated in the previous Appendix and show that two orthogonal *uniformly coupled* asynchronous modes can be resolved into a new set of orthogonal modes, but completely *uncoupled*. This implies, even if any coupling exists, as long as it is uniformly distributed, our results can be explained by assuming uncoupled, asynchronous modes. Obviously, the measured $\Delta\beta$ will now include the effects of coupling.

If no mode coupling exists between the modes, i.e., $\kappa = 0$, then from (23) and (24)

$$\alpha = \frac{\Delta\beta}{2} z \tag{32}$$

and

$$\eta = \tan^{-1}\left(\frac{2\kappa}{\Delta\beta}\right) = 0 \tag{33}$$

Under these conditions, from (21) and (22),

$$E_x = \cos\theta e^{-j\alpha} \tag{34}$$

$$E_y = \sin\theta e^{+j\alpha} \tag{35}$$

We have shown in the previous Appendix that in the most general case $0 < \eta/2 < \pm\pi/2$, there exists an input polarization angle such that $\theta = -\eta/2$, for which the output polarization remains linear for all lengths. As shown in Fig. 10, if we rotate the coordinate system by $-\eta/2$, then the angle θ' in the new coordinate system is

$$\theta' = \theta + \eta/2 \tag{36}$$

But substituting (36) in (21) and (22), and writing the amplitudes along Ox' and Oy' as

$$E_x' = E_x \cos\eta/2 - E_y \sin\eta/2 \tag{37}$$

and

$$E_y' = E_x \sin\eta/2 + E_y \cos\eta/2 \tag{38}$$

Using eqs. (34) through (38) we can easily show that

$$E_x' = \cos\theta' e^{-j\alpha} \tag{39}$$

$$E_y' = \sin\theta' e^{+j\alpha} \tag{40}$$

Eqs. (39) and (40) are identical to (34) and (35) with θ being replaced by θ'. Thus the coupled orthogonal modes can be easily resolved in terms of uncoupled orthogonal modes. Obviously, although α remains the same as in (23), it can be defined as in (32) to include the effects of the nonzero coupling as

$$\alpha = \frac{\Delta\beta_e}{2} z = \sqrt{\left(\frac{\Delta\beta}{2}\right)^2 + \kappa^2}\, z \tag{41}$$

By substituting (36) in (29) we find the ratio of major to minor axis of output ellipse is now given by

$$R = \frac{1 \pm (1 - \sin^2 2\theta' \sin^2 2\alpha)^{1/2}}{\sin 2\theta' \sin 2\alpha} \tag{42}$$

Therefore excitation at the input polarization reference angle ($\theta' = 0$) for which $R \to 0$ or ∞, the output remains linearly polarized for all lengths. Then if we vary θ' at the input, eq. (42) represents the ratio of

axes of output ellipse. The orientation of the output ellipse is now given by

$$\psi = \frac{1}{2}\tan^{-1}\left[\tan 2\theta' \cos 2\alpha\right] - \eta/2 \tag{43}$$

REFERENCES

1. F. P. Kapron, N. F. Borelli, and D. B. Keck, "Birefringence in Dielectric Optical Waveguides," IEEE J. Quant. Electronics, *8* (1972), p. 222.
2. W. Eickoff and O. Krumpholz, "Determination of The Ellipticity of Monomode Glass Fibers from Measurements of Scattered Light Intensity," Electron. Lett., *12* (1976), p. 405.
3. R. A. Steinberg and T. G. Giallorenzi, "Performance Limitations Imposed on Optical Waveguide Switches and Modulators by Polarization," Appl. Optics, *15* (1976), p. 2440.
4. M. Born and E. Wolf, *Principles of Optics*, 5th ed., Oxford: Pergamon Press.
5. G. W. Tasker, P. Kaiser, W. G. French, J. R. Simpson, H. M. Presby, and L. L. Blyler, Jr., "Low-Loss, Single-Mode Fibers with Different B_2O_3-SiO_2 Compositions," Appl. Optics, to be published.
6. H. M. Presby, R. D. Standley, J. B. MacChesney, and P. B. O'Connor, "Material Structure of Ge Doped Optical Fibers and Preforms," B.S.T.J., *54*, No. 10 (December 1975), pp. 168–1992.
7. S. E. Miller, "Coupled Wave Theory and Waveguide Applications," B.S.T.J., *33*, No. 3 (May 1954), pp. 661–719.
8. V. Ramaswamy and R. D. Standley, "A Phased, Optical Coupler Pair Switch," B.S.T.J., *55*, No. 6 (July–August 1976), pp. 767–776.